DOE/ER/45183-7

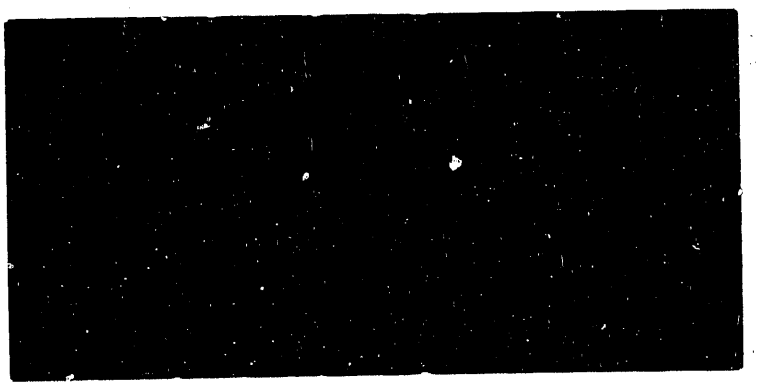

FOR

U.S. DEPARTMENT OF ENERGY

GRANT NO. DE-FG02-85ER45183

DOE/ER/45183--7

DE92 008110

PROGRESS REPORT FOR MATRIX GROUP

for

Materials Research and Beam Line Operation Utilizing NSLS

G. L. Liedl
Purdue University
West Lafayette, IN 47907

October 1991

Abstract

MATRIX, a participating research team of Midwest x-ray scattering specialists, continues to operate beam line X-18A at NSLS. Operations of this line now provides state-of-the-art capabilities to a wide range of people in the Materials Science and Engineering research community.

Improvements of the beam line continue to be a focus of MATRIX. Throughout this past year the emphasis has been shifting towards improvement in "user friendly" aspects. Simplified control operations and a shift to single-user personal computer has been a major part of the effort.

Over the past year the full 242 operational days were utilized. Beam line test and evaluation consumed 21 days with eight MATRIX groups combining to use 170 days. General user demand for use of the beam line continues to be strong and three groups were provided 51 operating days.

Research production has been growing as NSLS and the beam line become a more stable type of operation. For 1990 the MATRIX group published nine articles. To date for 1991 the same group has published, submitted, or has in prepartion twelve articles.

Among the milestones achieved last year one MATRIX member obtained the first data from a new ultra high vacuum chamber with low temperature capability. This is a unique capability at NSLS. Another member demonstrated grazing incidence small angle x-ray scattering capability for kinetic studies of film growth.

1.0. Introduction

The MATRIX Participating Research Team (PRT) was formed by people from some key midwestern institutions and includes people with overlapping interests in X-ray scattering. MATRIX is organized with an Executive Committee that establishes the policies for the operation of MATRIX. The Director of MATRIX has the responsibility for the administration of the operation in accordance with the polices of both the Executive Committee and NSLS.

MATRIX
Executive Committee
G. L. Liedl, Purdue University, Director
R. Colella, Purdue University
J. B. Cohen, Northwestern University
H. Chen, University of Illinois-Champaign-Urbana
H. Taub, University of Missouri-Columbia
Other Members,
S. Durbin, Purdue University
S. Ehrlich, Purdue University
P. Georgopoulos, Northwestern University

The MATRIX research effort is in PHASE TRANSFORMATION/CHARACTERIZATION where there are two major divisions of our activity related to the dimensionality of the problem, i.e., three dimension or two dimensional type problems.

2.0. Beam Line Projects

Over the past year emphasis has been on simplification and ease of operations. Also, efforts continue both to improve and to understand the beam line.

A new beam line manual was produced this past year and is attached as Appendix I. The manual includes not only a full description of the beam line but also some vital operating features. The manual is provided to all users and will be updated each year when new results are obtained on beam line operational features.

A primary focus for the coming year is to provide a full range of beam line control and data collection features. A coordinated plan includes a software manual and on-line operations help files.

3.0. Beam Line Utilization

Over the past year 242 operational days were available. The following table shows how these days were utilized. As in the past our practice involves the controlled development of the beam line and we reserve some time for such tests. Part of the 21 operational days assigned to the beam line are for tests and a small part is scheduled for changes in beam line configuration. All eight MATRIX members used some time last year and the distribution is as shown below. Our general user requests normally exceed the 25% allotment and we try to satisfy them. Last year three different groups were accommodated and given the days as indicated below.

MATRIX Beam Line Schedule
Sept. 14, 1990 Through August 31, 1991

Activity	Affiliation	Operational Days
Beam Line Tests		21
MATRIX Members		170
H. Chen	U. of Illinois	23
J. Cohen	Northwestern	9
R. Colella	Purdue	26
S. Durbin	Purdue	19
S. Ehrlich	MATRIX	28
P. Georgopoulos	Northwestern	5
G. Liedl	Liedl	27
H. Taub	U. of Missouri	33
General Users		51
Martines-Maranda		11
Ketterson	Northwestern	30
Dennison		10
	Total	242

PROGRESS REPORT

4.0. Research Milestones of Matrix Research Projects

Phase Characterization/Transformation - 3D

Liedl, et al: Early Stages of Phase Formation in Al-Li Alloys

The first early stage structural characterization of δ' precipitation in Al-Li alloys was completed. large amounts of the phase exist in the as-quenched state with increasing amounts on aging. Prior speculation was for a pure coarsening system following a spinodal decomposition. Our results indicate a simple nucleation and growth in the early stages. state with increasing amounts on aging.

Durbin, Ehrlich, et al: Anomalous X-Ray Scattering for Dopant Site Occupancy

Anomalous x-ray scattering experiements were made polycrystalline samples of lanthanum strontium cuprate with and without dopants of nickel and zinc. The site occupancy determination of the nickel and zinc was the primary goal. Fluorescence EXAFS was first done to allow calculation of complex structure factor as a function of energy. Anomalous scattering effects from measurements made above and below absorption edges provide maximum sensitivity in locating site occupancies in these complex oxides.

Phase Characterization/Transformation - 2D

Taub, et al: New UHV Chamber Operational

During April and May, 1990 we obtained our first x ray diffraction data from xenon films adsorbed on a single-crystal Ag(111) surface using the new MATRIX ultra-high vacuum chamber. The chamber is currently the only one at the NSLS with a low-temperature capability ($T \geq 30$ K). It also features in *in-situ* LEED system which allows LEED patterns to be obtained while the sample is located at the x ray scattering position. In the current experiment, the LEED system is used to establish the coverage corresponding to a complete xenon monolayer and bilayer. The purpose of the experiment is to study the structure and layer-by-layer growth of a relatively simple film physisorbed on a well-characterized single-crystal substrate. With x rays, we were able to measure the lattice constant of the xenon bilayer and multilayer films which had been inaccessible in previous LEED experiments. We also observed nucleation of bulk Xe crystallites following multilayer adsorption. This provides the strongest evidence to date that Xe incompletely wets the Ag(111) surface.

Taub, et al: X-Ray Diffraction and Scanning Tunneling Microscopy Studies of a Liquid Crystal Film Adsorbed on Single-crystal Graphite

Recently, there has been considerable activity in applying scanning tunneling microscopy (STM) to structure determinations of solid organic monolayers. We have developed techniques for using both STM and synchrotron x ray diffraction to probe the structure of the *same* organic film adsorbed on a single-crystal substrate. Our experiments have revealed a new commensurate monolayer phase of one of the most extensively investigated films--10CB (10-alkylcyanobiphenyl) molecules adsorbed on the graphite (0001) surface. We find a 10% discrepancy in the monolayer d-spacing inferred by x-ray and STM techniques. Our results are consistent with two generic structures of *n*CB monolayers on surfaces of hexagonal symmetry.

Cohen, et al: Graging Incidence Samll Angle X-Ray Scattering

The growth during deposition and during post-deposition annealing of gold islands 40-80 Å in diameter on glass substrates have been examined quantitatively and in situ with grazing incidence small angle x-ray scattering (GISAXS). This technique is a surface sensitive adaptation of small angle x-ray scattering and is non-destructive. These studies have been done in situ and non-destructively. The average island sizes and center-to-center island spacings have been determined as a function of gold coverage and annealing time and temperature. The annealing kinetics do not exhibit a power law depencence of average island size on time. Instead, the data is best described by a soft impingement, diffusion limited, island mobility dominated growth model. This model yields a quantitative signature for island mobility. The activation energy and diffusion coefficient for the island mobility growth process are found to be of the same order of magnitude as values for single atom surface diffusion.

5.0. Research Output

The impact of the MATRIX group is evident from the publications related to the use of the beam line. As NSLS and the beam line have become more dependable the research output has increased as seen from the table below.

Research Output

Year	1984	85	86	87	88	89	90	91
No. Publications	4	6	4	5	10	8	9	12
No. Theses	-	-	3	-	3	2	1	1

6.0. Publication Citations for 1989 and 1990
(Most Recent Reprints for 90 and 91 are given in Appendix II)

1989

1. W. Minor, L. D. Chapman, S. N. Ehrlich and R. Colella, "Phason Velocities in TaS_2 by X-ray Diffuse Scattering," Phys. Rev. B39, pp. 1360-1363, 1989.
2. Y. M. Koo and J. B. Cohen, "The Structure of GP Zones In Cu-10.9 at % Be" Acta Metall, Vol. 37, No 5, pp. 1295-1306, 1989.
3. J. D. Westwood and P. Georgopoulos, "A Maximum Entropy Method of Determining the Partial Distribution Functions of Multicomponent Amorphous Materials," J. Non-Crystalline Solids, 108, pp. 169-179, 1989.
4. D. R. Haeffner and J. B. Cohen, "X-Ray Diffuse Scattering Study of G. P. Zones in Al-4 at. % Zn," Acta Metall. 37, No. 8, pp 2185-2195, 1989.
5. R. Colella, J. R. Buschert, J. Z. Tischler, D. M. Mills and Q. Zhao, "Time Resolved X-ray Diffraction Study of Laser Annealing in Silicon at Grazing Incidence." Journal of Applied Physics, 66, p. 3523, 1989.
6. J. R. Levine, J. B. Cohen, Y. W. Chung and P. Georgopoulos, "Grazing Incidence Small-Angle X-ray Scattering: New Tool for Studying Thin Film Growth," J. Appl. Cryst. 22, pp. 528-532, 1989.
7. B. D. Butler and J. B. Cohen, "Diffuse X-ray Scattering Study of Cu_3Au Above the Order-Disorder Transition Temperature," Mat. Res. Sco. Symp. Prac. Vol. 138, pp. 59-64,(1989).
8. B. D. Butler and J. B. Cohen, "The Structure of Cu_3Au Above the Critical Temperature," J. Appl. Phys., 65, pp. 2214-2219, (1989).

1990

1. L. D. Chapman, S. N. Ehrlich and N. M. Lazarz, "A Time Resolved X-ray Scattering Technique for Observation of Non-Equilibrium Phonons," Rev. of Sci. Inst., Vol. 61, pp. 86-89, (1990).
2. B. J. Shaiu, H. T. Li, H. Y. Lee, and Haydn Chen, "Decomposition and Dissolution Kinetics of δ′ Precipitation in Al-Li Binary Alloys," Metallurgical Transactions A, Vol. 21A,: pp. 1133-1141, (1990).

3. Haydn Chen, J. Anderson, K. Ohshima, H. Okajima and J. Harada, "Atomic Short-Range-Order Structure in Au-Fe Alloys," Physical Review B, Vol. 42, 4, pp. 2342-2346 (1990).

4. R. Colella and Q.Shen, "Visibility of the Asymmetry Effect in Multiple Diffraction Experiments in Benzil. Wavelength Dependence" Acta Cryst. A46, 714 (1990).

5. J. B. Cohen, "X-ray Diffraction Studies of Catalysts, Ultramicroscopy, 34, pp. 41-46, (1990).

6. J. P. Anderson, Haydn Chen, and J. E. Epperson, "The Short-Range Order Structure of An As-Quenched Ni-12.5 at. % Si Alloy- A Synchrotron X-Ray Diffuse Scattering Study," Submitted to Acta Metallurgica (1990).

7. R. Colella, and Q. Shen, "Solution of the Phase Problem Using Multiple Bragg Scattering in a Protein Crystals," International Union of Crystallography, Invited Paper, (1990).

8. Q. Zhao, Q. Shen, S. Durbin and R. Colella, "Observation of Satellite Reflections in Potassium by High Energy Synchrotron X-Rays," Physical Review B, submitted (1990).

9. J. M. Chen, X. Q. Yang, D. Chapman, M. Nelson, T. A. Skotheim, S. N. Ehrlich, R. B. Rosner and M. F. Rubner, "Temperature Dependent Structure of Conducting Langmuir Blodgett Films Studied by X-ray Scattering," accepted by Molecular Crystals and Liquid Crystals.

1991

1. Joanne R. Levine, J. B. Cohen and Y. W. Chung, "Thin Film Island Growth Kinetics: A Grazing Incidence Small Angle X-ray Scattering Study of Gold on Glass," Surface Science, 248, pp. 215-224, (1991).

2. S. A. Hoffman, C. Venkatraman, S. N. Ehrlich, S. M. Durbin, and G. L. Liedl, "Structural and Transport Measurements in $La_{1.8}Sr_{0.2}NiO_{4+\delta}$," Physical Review B, 43, 10, pp 7852-58 (1991).

3. J. P. Quintana, B. D. Butler, and D. R. Haeffner, "Experimentally Determined Anomalous Scattering Factors for Mn, Fe, Cu, Zn and Hg Using the Kramers-Kronig Relation," J. Appl. Cryst., 24, pp. 184-187 (1991).

4. J. P. Quintana, "Practical Equation for Deadtime Determination in X-ray Counting Systems," J. Appl. Cryst., 24, pp. 261-262 (1991).

5. K. Mahalingam, V. Mahadev, G. L. Liedl and T. H. Sanders, Jr. "Precipitation Behavior of δ' in a Binary Al-Li Alloy," Script Met, 25, pp. 2181-86 (1991).

6. S. N. Ehrlich, L. D. Chapman and N. M. Lazarz, "Time-Resolved X-ray Diffraction of Hot Phonons in Quartz," in preparation.

7. P. Dai, S.-K. Wang, H. Taub, J. E. Buckley, S. N. Ehrlich, J. Z. Larese, G. Binning and D. P. E. Smith, "X-ray Diffraction and Scanning Tunneling Microscopy of a Liquid Crystal Film Adsorbed on Single-Crystal Graphite," in preparation for Phys. Rev. Lett.

8. J. M. Bloch, S. N. Ehrlich, A. S. Bommannavar and X. Yang, "Metal Ion Segregation to a Langmuir Monolayer," in preparation.

9. V. Mahadev, K. Mahalingam, G. L. Liedl, and T. H. Sanders, Jr., "Early Stage Precipitation in Al-Li Binary Alloys," in preparation.

10. R. Colella, "X-Ray Diffraction Studies of Surface Structures," Part I and Part II. Invited review article. To be published in Landolt-Bornstein, Volume III/24: "Physics of Solid Surfaces." Edited by G. Chiarotti (Springer-Verlag).

11. R. Colella, "Transaction Rod Scattering: Analysis by Dynamical Theory of X-Ray Diffraction." to be published, Phys. Rev. B.

12. R. Buschert and R. Colella, "Photostriction Effect in Silicon Observed by Time-Resolved X-Ray Diffraction." Submitted.

13. J. R. Dennison, S.-K. Wang, P. Dai, T. Angot, S. N. Ehrlich and H. Taub, "Ultra-high Vacuum Chamber for Synchrotron X-ray Diffraction from Films Adsorbed on Single-crystal Surfaces," in preparation for Rev. Sci. Instrmts.

14. J. P. Anderson, Haydn Chen and J. E. Epperson, The Atomic Short-Range Order Structure of a Water-Quenched Ni-12.5at.% Si Alloy - A Synchrotron X-ray Diffuse Scattering Study," in print, Met. Trans. (1991).

Appendix I
Beam Line Manual

MATRIX X-18A

BEAM LINE MANUAL

The purpose of this manual is to give an overview of the MATRIX X-18A beam line. Major components of the beam line, the diffractometer, detectors, the computer, motor indexers and drivers, etc., are described. Some advice about using the beam line is also provided. Appendices include measurements which have been made on the characteristics of the beam line. More detailed information about systems and components such as detectors, electronics, etc. can be found by reading the appropriate manuals. Computer software information is available through on-line help files and manuals.

TABLE OF CONTENTS

THE BEAM LINE

Introduction

The X-18A MATRIX beam line is shown in Figure 1. For the purpose of this manual the X-18A beam line starts at the isolation valve just outside of the shield wall and ends at the Be window located just in front of the hutch. The major components of the beam line are the fixed aperture, the first Be window, the horizontal and vertical slits, the monochromator, the mirror and the second Be window. There are also two fluorescent paddles, one after the monochromator and one after the mirror, which are used for alignment and diagnostic purposes. The hutch slits assembly will also be included in this section since it is physically attached to the end of the beam line. The total distance from the source to the sample position is 23500 mm.

The beam line is pumped by five ion pumps, one on the front end, one near each of the slits and mirror chambers, one under the monochromator chamber and one at the end of the beam line. There are three gate valves to allow different sections of the beam line (each with its own ion pump) to be bled up to atmosphere without affecting the rest of the beam line.

There are four parts of the beam line which are water-cooled because they are exposed to the white beam. These are the front end fixed aperture, the first Be window, the horizontal and vertical slits and the first crystal of the monochromator. The first three are cooled using the cooling water provided by NSLS while the first monochromator crystal is

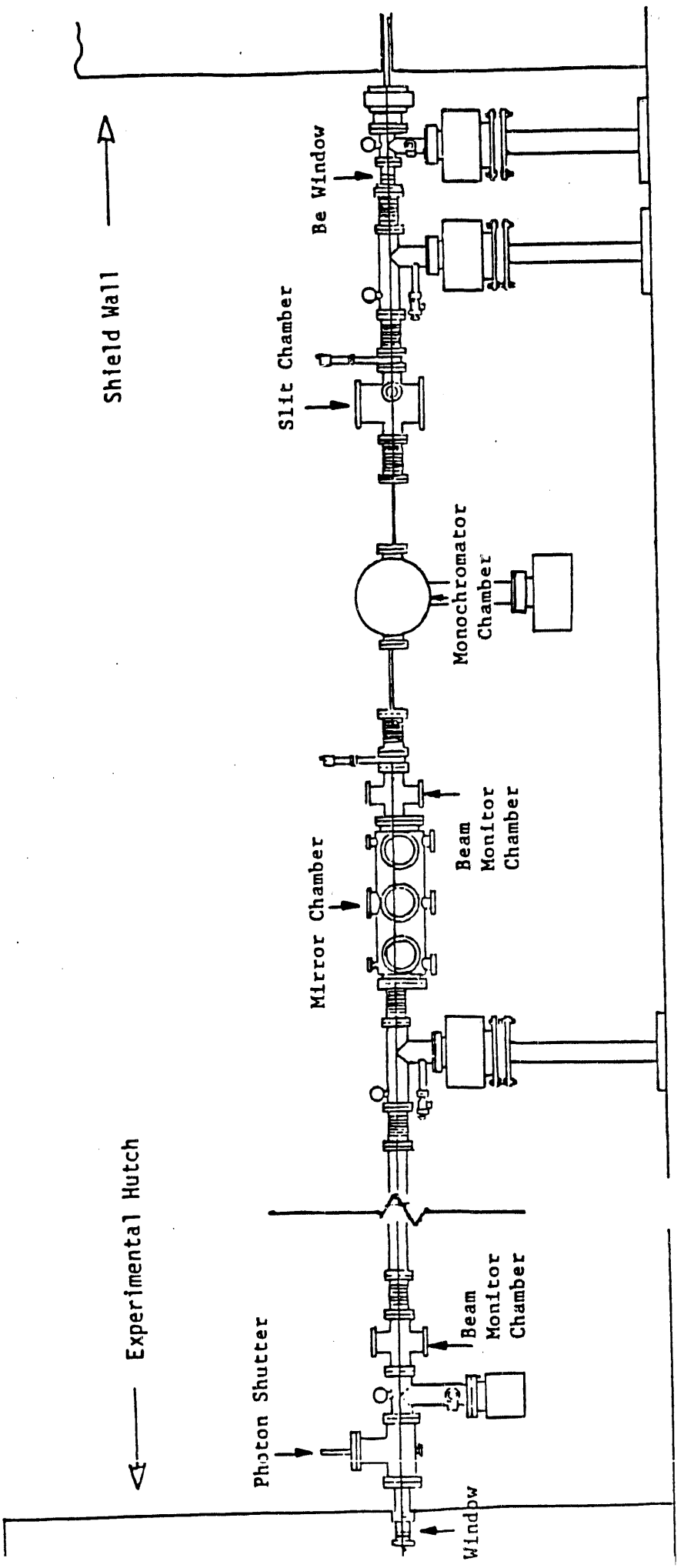
Shield Wall
Be Window
Slit Chamber
Monochromator Chamber
Beam Monitor Chamber
Mirror Chamber
Beam Monitor Chamber
Photon Shutter
Experimental Hutch
Window

Figure 1

cooled by our own water chiller to maintain it at a constant temperature. The water flow to each of these components is monitored by a Proteus flow switch.

Beam line safety requirements include the control and display of critical vacuum pressure and cooling water flow. The status of each of the five ion pumps (whether they are on or off), the water flow to each of the water-cooled components (whether the flow rate is above or below a set point), and the status of the isolation valve (whether it is fully open or not) is displayed on the panel just to the right and above the hutch door. All of the green lights should be on. If there is a fault anywhere the red light associated with that component will go on (the green light will go off) and the saftey shutter in the front end will automatically close. The safety shutter must be opened by the user and can only be done so if the panel shows all green lights again. If any red light goes on PLEASE NOTIFY THE MANAGEMENT so that the problem can be fixed.

The fixed aperture is used to cut the horizontal fan of the beam from 8 milliradians (dictated by the front end aperture) down to 6 milliradians so the beam can pass through the first Be window. The fixed aperture is 7682 mm from the source. The first Be window is 5 mm high, 50 mm wide and 10 mil thick. It is located 7998 mm from the source. When the isolation valve is closed it separates the X-18A beam line vacuum from the front end vacuum, which is connected to ring vacuum and is shared by both X-18A and X-18B. The beam line vacuum is contained at the end of the beam line by the second Be window which is 1 inch in diameter and 10 mil thick, and is located just outside the hutch.

The Beam Line Slits

The beam line slits are the first major components of the beam line which can be adjusted by the user. They are located 9127 mm from source point. We have both horizontal and vertical slits in the chamber and a viewport so we can see where the x-ray beam hits the slits (they are coated with fluorescent powder). The horizontal slit is an upside down V which lets about 6 mrad through at the bottom and goes to zero at the top. The vertical slit is a set of 6 slits of heights 4 mm, 3 mm, 2 mm, 1 mm, 0.6 mm and 0.3 mm, going from bottom to top. They can both be moved manually by turning a crank attached to a mechanical actuator on top of the slits chamber.

The vertical cross-section of the white beam coming through the first Be window was mapped by placing a detector at the end of the beam line and scanning the 1 mm high vertical slit of the beam line slits assembly through the beam at two energies, 8 keV and 15 keV. A plot of these scans is shown in Figure 2. Note that the hot part of the beam is in the center of the whole beam getting through the first Be window (the peaks are symmetric).

The beam line slits have several uses. When the focusing mirror is being used the angular dispersion of the beam is increased leading to poorer resolution. This loss in resolution can be lessened by narrowing the beam in the horizontal direction so that the beam is reflecting off less of the sides of the cylindrical mirror and more off the center of the cylinder. This, of course, will also cut down on the intensity of the beam reaching the sample, so a compromise must be reached.

When the beam line slits are 'wide open' the beam is larger than the cross- section of

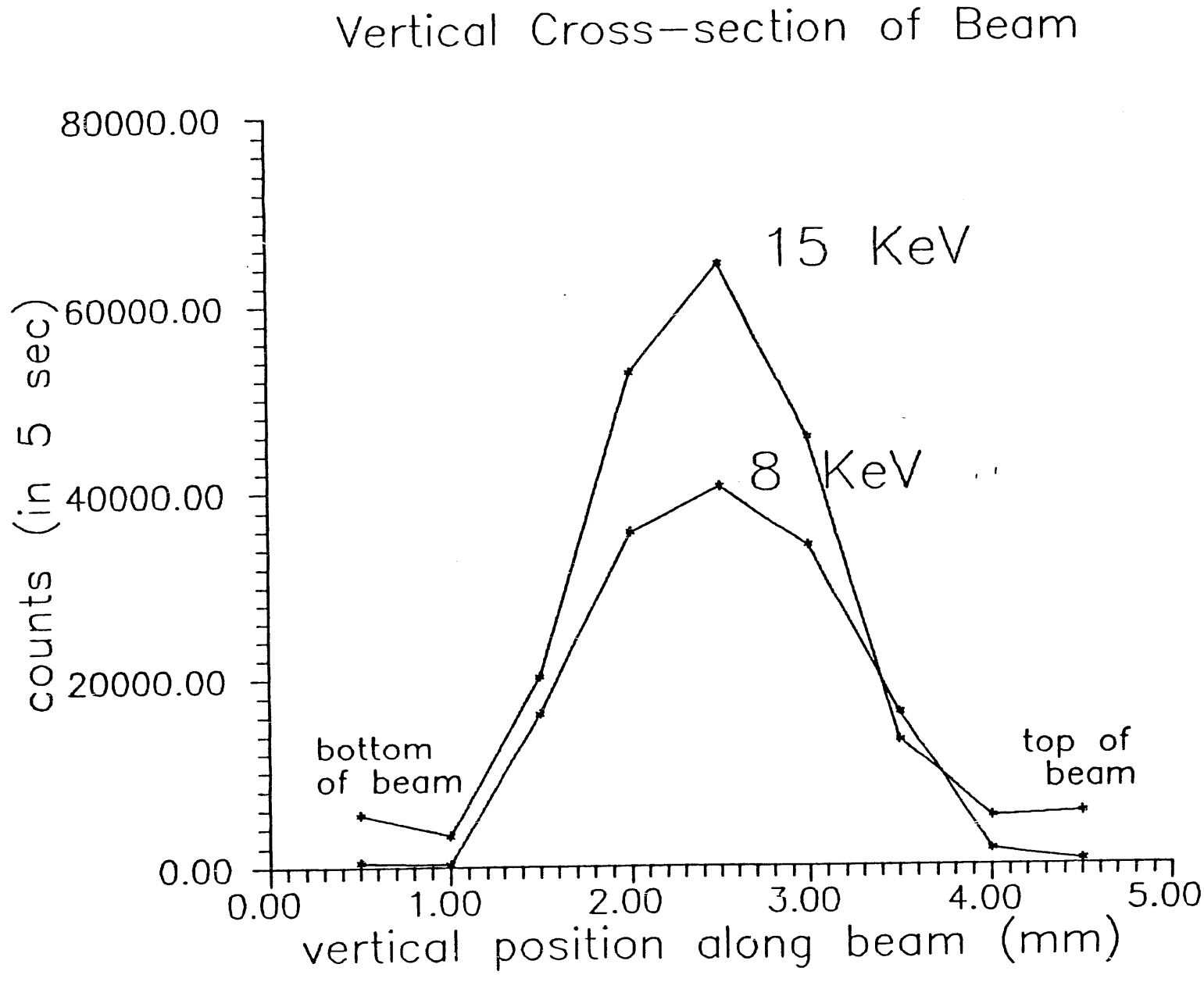
Vertical Cross-section of Beam
80000.00
60000.00
40000.00
20000.00
0.00
counts (in 5 sec)
15 KeV
8 KeV
bottom of beam
top of beam
0.00
1.00
2.00
3.00
4.00
5.00
vertical position along beam (mm)

Figure 2

the mirror so some radiation can get down the beampipe and reach the sample. This 'stray' radiation may contain some higher harmonics which the mirror is meant to diminish. The beam line slits should therefore be adjusted appropriatedly if these effects are important.

The Monochromator

The X-18A monochromator is located 10117 mm from the source. It has two Si (111) crystals and has an energy range of about 4.0 - 20 KeV. It is not a fixed exit geometry and thus the beam is low at lower energies and high at higher energies. The relative height of the beam exiting the monochromator as a function of energy is shown in Figure 3.

The angle of the two crystals with respect to the beam is adjusted by a Huber circle which is external to the monochromator chamber, and is connected to the crystal mounts by a tubular support which seals with the chamber using two Viton o-rings. The first crystal of the monchromator is cooled by water circulated through a chiller located under the beam line. The inside of the monochromator can be seen through a viewport on the X-18B side.

The fine adjustment of the second crystal angle and tilt is accomplished through two piezoelectric crystals by applying a voltage of between 0 and negative 1000 volts to each of them. The dual high voltage supply used is the one with the red LED readouts. Since these supplies are only capable of supplying a voltage of up to 1000 volts it is tough to apply too much voltage to the piezoelectric crystals. However, when using these it is important to touch only the voltage adjust knobs. DO NOT CHANGE THE POLARITY

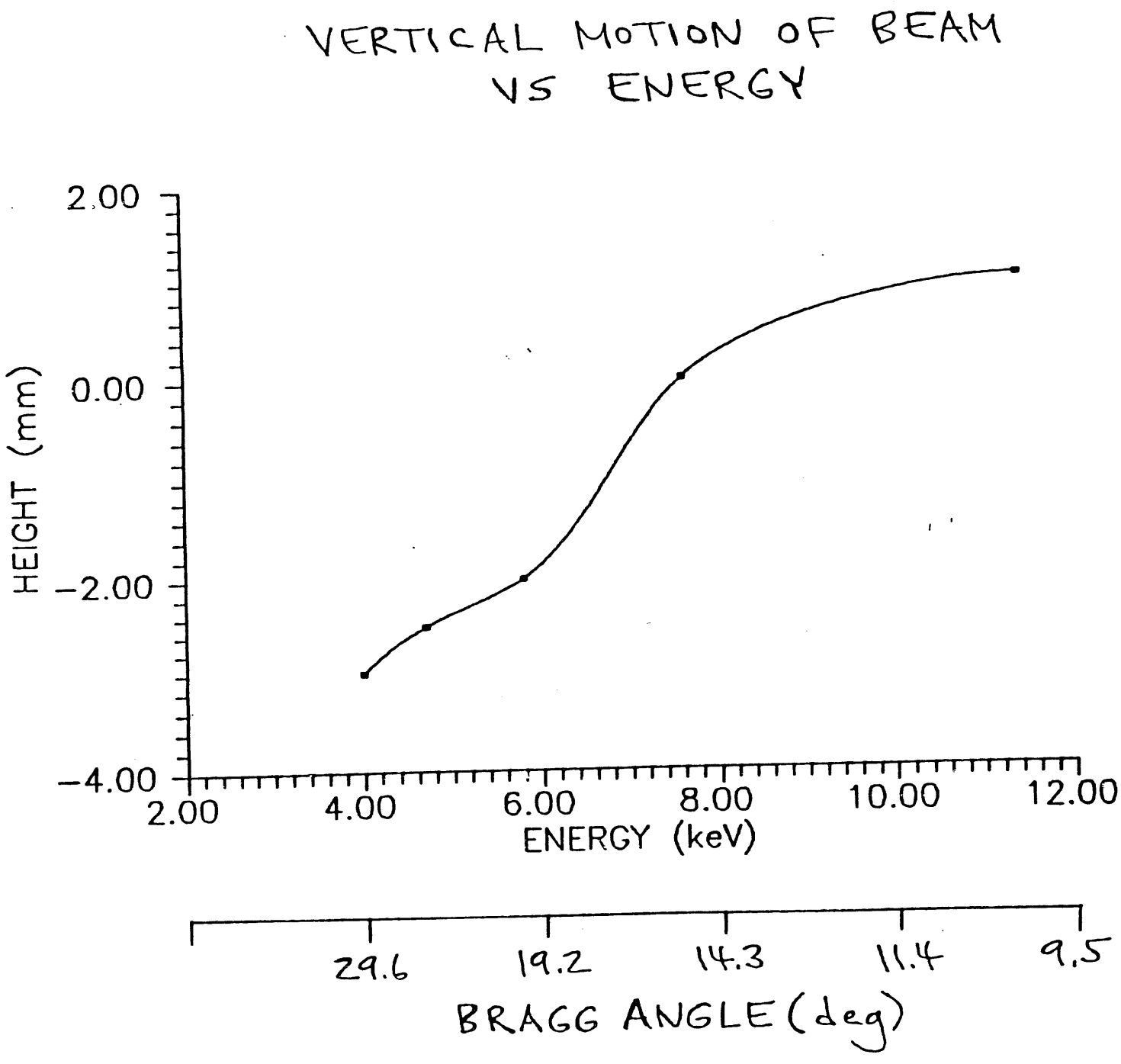
VERTICAL MOTION OF BEAM
VS ENERGY
2.00
0.00
−2.00
−4.00
HEIGHT (mm)
2.00
4.00
6.00
8.00
10.00
12.00
ENERGY (keV)
29.6
19.2
14.3
11.4
9.5
BRAGG ANGLE (deg)

Figure 3

OF THESE HIGH VOLTAGE SUPPLIES TO POSITIVE AND DO NOT CONNECT THE PIEZOELECTRIC CRYSTALS TO ANY OTHER HIGH VOLTAGE SUPPLY.

When changing energy by more than a keV it is usually necessary to finely adjust the angle of the second monochromator crystal using the top half of the dual high voltage supply in order to peak the intensity. If you are changing the angle of the monochromator crystals by many keV it is usually a good idea to change the angle in steps, finely adjusting the angle of the second crystal with the piezoelectric crystal to peak the intensity as you change energy so you never lose the beam.

Adjusting the tilt of the second monochromator crystal has the effect of moving the beam horizontally in the hutch (there doesn't seem to be much loss in intensity when doing this). The two crystals are parallel only at a certain tilt voltage. When this condition is achieved the beam will stay fairly stationary in the horizontal direction as the energy is changed over its entire range. If the crystals are not parallel then as you change the energy the beam will move horizontally. Therefore if you are planning on changing the energy during the course of your experiment it is important that the tilt of the second crystal be parallel to the first, otherwise the beam will surely move sideways. The easiest way to do this is to view the beam, using the TV monitor, on a fluorescent screen placed at the sample position. Mark the position of the beam on the monitor at the lowest energy you are planning to use. Change the energy to the highest you are planning to use and make sure the beam hasn't moved from the mark you made on the TV monitor. This alignment is checked regularly by the management, but should be checked if it is important.

The calibration of the monochromator has been made in several ways. Details of this are contained in Appendix A. If you have any questions about the calibration of the

monochromator please ask, or measure it yourself. However, DO NOT CHANGE THE CALIBRATION OF THE MONOCHROMATOR ON THE COMPUTER. THIS IS TO BE DONE BY THE MANAGEMENT ONLY.

The Mirror

The X-18A mirror is located 11750 mm from the source. It is a cylindrical aluminum mirror which is electroless nickel-plated and then coated with platinum. It is 700 mm long, 100 mm wide and 44 mm high. The radius of curvature of the cylinder is 78 mm. The width of the cylinder at the top of the mirror is 78 mm. The mirror is designed to focus the source point of the synchrotron at the sample position. The cylindrical shape of the mirror focuses the beam horizontally while focusing in the vertical is achieved by bending the mirror along its length. The mirror sits 11750 mm downstream of the source point and the same distance upstream of the sample position, making the total length of the beam line from source to sample 23500 mm. The mirror is designed to focus at the sample with an incident angle of about 6.6 milliradians. This makes the cutoff energy about 12 KeV.

In order to use the beam line focusing mirror the Be window at the end of the beam line must be raised so that the beam reflected up from the mirror can still pass through it. The standard configuration of the beam line is with the focusing mirror in place. Those who do not wish to use the mirror must request this change in normal beam line configuration before the schedule is made. In this way, those not using the mirror can be scheduled consecutively, and time can be scheduled for raising the beam line, refocusing the mirror and realigning the diffractometer.

Mirror Support

The mirror is supported at two points, at the upstream end and at the downstream end. Each of these supports has a vertical and horizontal motion. In addition, the mirror can be bent along its length.

Vertical Motion

The vertical motion of each mirror support can be used to adjust the height and the angle of the mirror with respect to the beam. The vertical motion is achieved by mounting each end of the mirror on a vertical slide which is then supported by a mechanical actuator (1 turn = 0.0254 mm travel) mounted on the bottom of the mirror support frame. A stepping motor is fastened to the worm of each mechanical actuator so that the vertical motion of the mirror can be controlled by the computer.

Horizontal Motion

The horizontal motion is used to align the mirror so that its length is parallel to the beam. The horizontal motion is achieved by mounting each end of the mirror on a horizontal slide (which is then mounted on the vertical slide above). The motion of each of these slides can be controlled by a micrometer (1 turn = 0.5 mm travel), which can then be locked. This motion is used only when aligning the mirror and SHOULD ONLY BE TOUCHED BY THE MANAGEMENT.

Mirror Bending

The mirror is bent along its length in order to focus the beam vertically. Each end of the mirror is bent independently. A lever arm is attached to the yoke in which each

end of the mirror sits. By moving the opposite end of the lever arm down, a torque is applied to the end of the mirror causing it to bend. A linear feedthrough on each end of the mirror support is used to move the lever arm attached to the opposite end of the mirror, thereby bending or not bending it. When not bending the mirror it is supported freely on each end with no torque being provided by the lever arms, but it may still bend under its own weight. THE BENDING OF THE MIRROR SHOULD ALSO BE DONE BY THE MANAGEMENT ONLY.

The Hutch Slits Assembly

At the end of the beam line is a 1 inch diameter, 10 mil thick Be window. Just after this window is the hutch slits assembly. It is kept evacuated by the pump inside the hutch. The assembly can be fit with extensions of different lengths to bring this vacuum within different distances of the sample position. A set of four slits, two vertical and two horizontal, inside this assembly can be adjusted by external stepping motors. The center and separation of both vertical and horizontal pair of slits can be moved and scanned by the computer. A scintillation detector is attached to the bottom of this assembly for use as a monitor of the incident beam intensity. X-rays for this monitor detector are provided by passing the incident beam through a 1 mil thick piece of Kapton inside the assembly, placed 45° to the beam. The window at the end of this assembly is 1 inch diameter, 3 mil thick Kapton.

THE HUTCH

The hutch provides space for all experimental equipment. Standard equipment includes the diffractometer, diffractometer support table, special chambers to be mounted on the diffractometer, detect rs, and the He-filled detector path.

The Diffractometer

The diffractometer is a 6-circle Huber model. The 6 circles are χ, ϕ, θ (ω), 2θ, and θ and 2θ for the analyzer. The diffractometer is shown in Figure 4.

The first four motions are used most often and are controlled by the microsteppers. The χ, θ and 2θ motions are geared so that 1 revolution of the motor corresponds to 1° of motion. The ϕ motion is geared so that 1 revolution of the motor corresponds to 2° of motion. The microsteppers are currently splitting up one revolution of these motors into 20,000 steps.

The zeroes of the diffractometer motions are defined as follows. $\chi = 0$ when the ϕ mount is opposite to the θ table and the ϕ axis is parallel to the θ and 2θ axes. $\theta = 0$ when the plane of the χ circle is perpendicular (χ-axis is parallel) to the incoming beam. $2\theta = 0$ when the 2θ detector is receiving the incoming beam.

The sense of these motions is as follows. If we look at the diffractometer with the incoming beam coming from the right, θ and 2θ move in the positive direction when they move clockwise. If we look at the diffractometer with the incoming beam coming towards

us, χ moves in the postive direction when it moves clockwise. When $\chi = 0$, ϕ moves in the positive direction when it moves in the opposite direction of θ.

The analyzer θ and 2θ motions are geared so that 20 revolutions of the motor correspond to 1° of motion. These motions are controlled by standard motor drivers which split up one revolution of the motor into 400 steps (half-step mode).

Aligning the Diffractometer

The following is just one way of aligning the diffractometer in χ, θ and 2θ with the beam. It makes use of the Soller slits, which mount on the sample goniometer. Steps 1)–3) ensure that the incident beam hits the center of the diffractometer. Steps 6)–10) ensure that the plane of the χ circle is perpendicular to the beam.

1) Mount goniometer and cone on ϕ mount and center in Huber using scope. This is accomplished when the point of the cone remains stationary in the scope when first spinning ϕ and then χ. Note that it is not necesssary for the point of the cone to be centered in the crosshairs of the scope, just that it remain in the same place while spinning ϕ and χ. Occasionally the scope gets banged or moved somehow so that the crosshairs are not still centered on the center of the diffractometer. When this happens please notify the management so that this can be fixed.

2) Choose incident beam size with slits and center around hot spot of beam. This is assuming that the mirror has already been focused at the sample position. The slit size, both vertical and horizontal, can then be set and the slits can be scanned both in the vertical and horizontal so that they are centered on the brightest part of the beam. The monitor detector can be used to collect counts as a function of time while

doing this. Note that, since the beam is being focused, the beam size at the sample position may not be the same as the incident beam slit size. Measure beam size at the sample position.

3) Center cone (and therefore Huber) in beam using using fluorescent screen, x-ray paper and diffractometer table motions.

4) Mount ion chamber on 2θ arm and place in position to accept beam (make sure detector slits are open wide enough).

5) Mount Soller slits on goniometer so that at $\chi = 0$ the blades of the Soller slits are horizontal. Make sure beam is hitting Soller slits.

6) Do a ϕ scan at $\chi = 0$. Move ϕ to where peak is and set $\phi = 0$ there.

7) Move to $\chi = 180°$ and do another ϕ scan. If peak is at ϕ' move to $\phi'/2$.

8) Do a θ scan. There should be a peak at $\pm\phi'/2$. Move to where θ scan shows a peak and set $\theta = 0$ there. Check at $\chi = 0$.

9) Now go to $\chi = 90°$ so that the blades of the Soller slits are vertical. Do a ϕ scan. Move ϕ to where peak is and set $\phi = 0$ there. Move to $\chi = 270°$ and do another ϕ scan. If peak is at ϕ'' move to $\phi''/2$.

10) Do a scan with the diffractometer table yaw (rotation about the vertical). There should be a peak at $\pm\phi''/2$. Move to where the table yaw shows a peak and leave it there.

The χ zero can be found in two ways.

11) The first way is to just put a level on the ϕ table and adjust χ so that the ϕ table is level. This is then $\chi = 90°$.

12) The second way is more complicated. Move to $\theta = 90°$, $\chi \simeq 180$ and $\phi = 0$. Mount

the Soller slits in the sample goniometer so that the blades are vertical. Scan χ and find the peak position. Move χ to the peak position and set $\chi = 180$ there. Move to $\chi = 0°$. Scan χ again. If peak is at χ', move χ to $\chi'/2$ and set $\chi = 0$ there.

13) In order to find the 2θ zero first set the detector slits to final size. Scan 2θ to find the peak. Move to the peak postion and set $2\theta = 0$ there.

14) Set scatter slits a little larger than the detector slits.

15) Put x-ray paper before and after these pair of slits. Pictures should match so that these slits are in line with the incident beam slits.

Setting Limits on the Diffractometer

There are two types of limits which can be set on the χ, θ and 2θ motions of the diffractometer, hard limits and software limits (the ϕ motion and the 2 analyzer motions only have software limits). Hard limits (those small cylindrical things) are set to protect the diffractometer motions from running into other things or each other. Software limits should always be set so that they will be hit before a hard limit is hit. Therefore, if the software limits are set properly a hard limit should never be hit.

Hard limits should not be removed completely from the θ or 2θ motions. If it is necessary to move one, just loosen its screw, slide it along its path and then tighten its screw when it is in its new position. The χ motion generally does not have hard limits attached on a permanent basis.

There are two hard limits which are set on the 2θ motion and should not be changed. One prevents the 2θ arm from hitting the TV camera in the hutch and the other prevents it from hitting the diffractometer table. There is an additional one which can be set between

these two to prevent the 2θ arm from going to zero and thus allowing the detector to see the direct beam. In all cases a software limit should be set to prevent this from happening when either a scintillation or silicon detector is being used. A software limit should also be set just above the highest 2θ value which will be used.

The hard limits on the θ motion are generally set to prevent the χ circle from hitting the incident beam path. If the long extension on the incident beam assembly is being used this has already been set at 45°. If the long incident beam path is not attached and this is not a problem then they may be set to just beyond where the χ circle blocks the incident beam. Software limits should be set inside of the hard limits. If negative θ will not be used the lower software limit may be set close to zero. If a chamber or something similar is mounted on the diffractometer then these limits should be appropriately set to prevent collisions.

The hard limits on the χ motion are generally not needed unless a chamber or something similar is mounted on the diffractometer. However, software limits should be used to prevent the χ circle from turning more than 180° in either direction, less if possible. This is to prevent the ϕ motor cable form being pulled too much.

Software limits should be used for the ϕ motion if a chamber or something similar is mounted on the diffractometer to prevent collisions.

The status of the hard limits on the diffractometer and the monochromator (whether one has been hit or not) is indicated on the leftmost module in the top Nimbin in the equipment rack. A red LED will go on indicating which limit has been hit. A motion can be disabled completely by turning off the appropriate switch on this module. This has the effect of both limits on that motion being hit at once so that no motion can take place.

The Diffractometer Table

The diffractometer table supports the diffractometer and provides motions to place the center of the diffractometer in the incident beam. It consists of a top section which has five motors which provide motions for vertical height, yaw, pitch, roll and horizontal translation, all with respect to the beam. A lower table provides up to a 7 inch vertical translation for raising and lowering the diffractometer when using and not using the mirror.

The top section has a 3-point support, each which can be moved vertically by a combination of a 200 turns per inch mechanical actuator and a stepping motor. This section has a motor which rotates the table about a vertical axis passing approximately through the center of the diffractometer which is also controlled by the same mechanical actuator, stepping motor combination. There is also a motor which translates the table perpendicularly (and horizontally) to the beam. The 5 motions of the diffractometer table do not have hard limits but they do have software limits which have been set by the management.

These motors are used to provide the five motions of yaw, roll, pitch, vertical translation and horizontal translation for the diffractometer table.

1. Yaw - a rotation around a vertical axis passing through the center of the diffractometer. A positive yaw is in the counter-clockwise direction when viewing from above.
2. Roll - a rotation about a horizontal axis coincident with the beam. A positive roll is in the counter-clockwise direction when looking into the beam.
3. Pitch - a rotation about a horizontal axis perpendicular to the beam. A positive pitch is in the counter-clockwise direction when viewing from the door side of the hutch.

4. Vertical translation - the raising and lowering of the table, with positive being in the up direction.
5. Horizontal translation - a motion perpendicular to the beam with positive to the right when looking into the beam (away from the door side of the hutch).

The Detectors

The beam line has two Bicron and two Harshaw scintillation detectors, two PGT silicon detectors and two ion chambers. The Harshaw scintillation detectors are reserved for use as a monitor detector of the incoming beam (one is a spare). The ion chambers should be used any time very high count rates are to be measured, such as when looking at the direct beam.

The cables from the detectors for high voltage, signal and preamp power can be plugged directly into the panel to the right of the hutch door. The connectors on this panel are connected to the equipment rack, directly into the back of the lower Nimbin (or other) electronics. Other pieces of detector electronics are available in Cabinet 1.

The Bicron scintillation detectors should be used at a voltage of about +700 volts. They are generally connected to an amplifier and then to a single channel analyzer (SCA) (the amp and SCA may be combined into one module). The windows of the SCA should be reset anytime the energy of the x-rays is changed. The output signal from the SCA can then be fed into a counter and a ratemeter. The signal from the amplifier is generally fed also into the oscilloscope for observing the voltage pulses coming from the detector.

The PGT silicon detectors must only be used at liquid nitrogen temperature or damage to them can result. The beam line has a liquid nitrogen dewar for this purpose. THEY MUST BE COOLED AT LEAST 6 HOURS BEFORE THEY ARE FIRST USED. They are used with the PGT high voltage supply SET SLOWLY TO −600 VOLTS FROM ZERO. Please read the instruction manuals or ask questions if you are not familiar with these detectors so that you will not damage them. They are very expensive to repair.

Other Equipment in the Hutch

He-filled Detector Flight Path

A beam flight path from the sample to the detector can be mounted on the 2-theta arm of the diffractometer and filled with helium. It is composed of two pieces, one which goes from the detector to the end of the dovetail and one which extends closer to the sample, and which can be removed by the management if it interferes with a sample or chamber mounted on the diffractometer. There is a 1 mil thick Kapton window on each end of the assembly. There is a set of slits mounted to the detector side of this flight path as well as a cowl into which the detector can fit to keep scattered radiation from entering it. The inside of the cowl is lined with plastic to keep it electrically isolated from the detector. A set of slits is usually mounted to the sample side of the flight path for use as scatter slits. The entire flight path is leaktight and can be filled with helium from a Polyflo tube which is hanging from the top of the hutch and is connected to a He tank strapped to the front of the hutch. The pressure of this He is usually kept at 1-1.5 PSI. The flight

path can be flushed with He by lifting up on the pressure relief valve on the sample side of the tube.

Diffractometer Accessories

There are pieces of equipment either inside of the hutch or in Cabinet 1 which can be used on the diffractometer. These include:

1) Soller slits
2) Ge(111) analyzer crystal
3) Silicon powder
4) highly ordered pyrolytic graphite (HOPG)
5) two large Huber goniometers which fit on the Huber phi mount
6) several aluminum sample mounts which fit on the goniometers above
7) lead foil for shielding
8) extra sets of Huber slits
9) goniometer extensions

If you can't find something please ask.

SUPPORT EQUIPMENT

The equipment in this section includes all that is normally located outside of the hutch. This includes motor indexers and drivers, computers and electronics stored in the equipment rack and elsewhere.

Motor Indexers and Drivers

Motors on the beam line are run by either the Superior Electric Modulynx microstepping and normal stepping indexers or digital I/O signals from a PC board (Real Time Devices, Inc., model DG24). The Modulynx microstepping indexers are running the 4 diffractometer motors, the monochromator motor and the diffractometer analyzer theta motor. The Modulynx normal stepping indexers are running the 5 diffractometer table motors and the diffractometer analyzer 2-theta motor. The PC board motor indexer is running the beam line slits motors, the mirror motors and the 4 hutch incident beam slits motors.

The microsteppers have given us few problems since the new beam line has been running. This is due to several steps which have been taken. The power lines to the driver cards are now fused so they will not be able to draw too much power from the power supply. Hard limits have been connected on the diffractometer and monochromator. In addition, there is a master enable-disable switch to the right of the hutch door which, when moved down, will close all the limit switches at once. There is also a module in the top Nimbin on the rack, labeled 'μSTEPPER STATUS', that indicates which hard limit

has been hit for the microsteppers and from which any of the microstepped motors can be disabled individually by turning off the appropriate switch (both red LEDs will go on). Finally, software limits can be set.

A second module to the right of the microstepper module, labeled 'MODULYNX STATUS', indicates the status (green LED for motor motion and yellow LED for direction) of the motors run by the Modulynx normal stepping indexers.

If any of the motors run by the Modulynx indexers refuses to move first check both software and hard limits. If this isn't the cause it is most likely a software problem or a blown fuse, either one in-line to the driver cards or the power supplies for the driver cards located at the bottom of the rack. Please notify the management if this happens.

The signals from the PC board motor indexer first run through a module on the right of the topmost Nimbin in the electronics rack. This module gives information about eight motors. The signals for motor motion and direction are indicated by the green and yellow LEDs, respectively. The red LEDs light up when a hard limit has been hit. The switch can be used to enable or disable a motor. Both red LEDs will light up when a motor is disabled. It is important to place the appropriate switch in the up position before moving the motors they are connected to. Please return the switch to the down position when you are finished moving these motors.

The drivers for the slits motors are mounted on the front wall of the hutch to the left of the TV camera. The drivers for the beam line slits and mirror motors are located in the third rack in front of the hutch. The power for these last drivers must be turned on using the switch to the left of the oscilloscope (the blue light will come on) before moving these motors. When not using these motors for a long period of time please turn off the

power to them.

Electronics

The electronics available at the beam line are listed below. Information about any of this equipment is available in equipment manuals in the beam line filing cabinet. Please realize that at any one time one or more of these may be out for repair. If any of them is crucial to your experiment please call before coming to Brookhaven.

Item	Quantity
Power Designs High Voltage Supply (0-3000V)	2
Ortec 556 High Voltage Supply (0-3000V)	2
PGT Bias Supply	2
GSK Scientific P11-10 (for ion chamber)	2
Tennelec TC246 AMP/SCA	3
Canberra 1718 X-Ray Amplifier Pulse Height Analyzer	1
Canberra 2020 Spectroscopy Amplifier	1
Ortec 672 Spectroscopy Amplifier	1
Ortec 460 Delay Line Amplifier	1
Canberra 2035A Constant Fraction Timing SCA	2
Ortec 550A SCA	1
Tennelec TC525 Ratemeter	2
Canberra 2081 Ratemeter	2

Ortec 974 Quad Counter Timer	2
Canberrra 2071 Dual Counter Timer	2
Tennelec TC535P Timer/Multi-Scaler	1
BNC DB-2 Random Pulse Generator	1
Ortec 495 Power Supply	1
Canberra 2000 Nimbin	1
Tennelec TB3 Nimbin	1
Tektronix 2215 60Mhz Oscilloscope	1
Hewlett-Packard HP3478A Multimeter	1

Pumps

We have several pumps available at the beam line. The small turbo pump can be used for pumping out the cryostat or other chambers requiring high vacuum. It has a connection for a Kwik-Flange 25 fitting. We have two small direct-drive two-stage rotary vane pumps for use in pumping on small chambers or anything else not requiring high vacuum. When using these pumps please make sure that your vacuum hoses are securely attached and your chamber is reasonably leaktight.

THE COMPUTER

There are two personal computers at the beam line. They are identical, each having an 80386-16 processor, an 80287 math coprocessor, 2 MB RAM, a 70 MB hard disk, a 1.2 MB 5.25 inch floppy drive, a 1.44 MB 3.5 inch floppy drive, a 60 MB tape tape backup and VGA graphics with a VGA color monitor. Both are connected to a 24-pin letter quality, dot matrix printer. One computer is used to control experiments (computer 1) while the other (computer 2) is a spare, and can be used for any other purpose.

The hard disk of each computer is partitioned into disks C and D. Disk C contains beam line and other software which can be used by users. No one but the management should touch disk C. Disk D on each computer has a directory for each user. All of your work should go into your directory on disk D.

Information about the beam line software is available in help files inside the software. Computer 1 also contains a multi-channel analyzer card which can be used to collect energy spectra from a detector. Computer 2 is connected to a box which provides access to the computer networks. We have an account on the NSLS Vax which can be used for e-mail. Please ask for directions on how to log onto this computer.

After finishing your experiment please remember to copy your data to bring home. Don't remove your data from the computer's hard disk. As a precaution, we make it a practice to back-up everyone's data onto their own tape cartridge after they leave. However, we only back-up data which we find in your directory in disk D of computer 1. So if you have data anywhere else and would like it backed up please move it to this location. These tape cartridges are kept at Brookhaven.

APPENDIX A

Monochromator Calibration

The calibration of the monochromator has been done in several ways and these different methods have been used to check each other. The first method used to calibrate the monochromator was to measure the (111) and (333) reflections of a small piece (about 1 mm diameter) of powdered silicon at three energies, ~6 keV, ~8 keV and ~12 keV. The peaks for these reflections are shown in Figures A1-A6. The wavelengths determined from these two reflections agreed within 0.001 angstroms for a given wavelength and by the same amount among the energies measured.

The second way the monochromator was calibrated was to measure the absorption edge of several elements. These are shown in Figures A7-A9.

There are two ways we have of measuring the angle of the monochromator crystals independent of the computer. The first way is with an optical encoder attached to the monochromator motor. This encoder has a resolution of 0.001 degrees. It is connected to a counter with an LED readout which is near the top of the equipment rack. The readout gives the angle of the monochromator crystals and can be compared to the angle of the monochromator crystals given by the computer at any time. The second way is by reading the dial on the monochromator Huber. This can be read to about 0.005 degrees. The dial readings at 1.556 Å(7968 eV) are 14.7° on the large scale and 43.1 on the small motor dial. THE MONOCHROMATOR CALLIBRATION ON THE COMPUTER SHOULD BE CHANGED ONLY BY THE MANAGEMENT.

APPENDIX B

Monitor Counts versus Energy

A measurement was made of the monitor counts per second versus the energy of the x-rays using the focusing mirror. This was done by changing the energy, then peaking the intensity by retuning the monitor detector SCA, the second monochromator piezoelectric crystals and the mirror. The counts were measured on a ratemeter and normalized to the ring current. The monitor detector is a scintillation detector looking at the scattered x-rays from a 1 mil thick piece of Kapton at 45 degrees to the incident beam. No attempt was made to correct for the energy dependence of the x-ray scattering from the Kapton. This measurement is shown in Figure B1.

Notice the intensity dying off at about 12 keV, the energy cutoff of the mirror. The large dip at about 8.5 keV is somewhat of a mystery and may be due to absorption from the electroless Ni plating underneath the Pt coating on the mirror. This dip is not seen without the mirror in place.

This plot is meant to be an aid in choosing an x-ray energy at which to work. If the energy used is not critical and intensity is important, it may be wise to work at an energy which gives the most intensity.

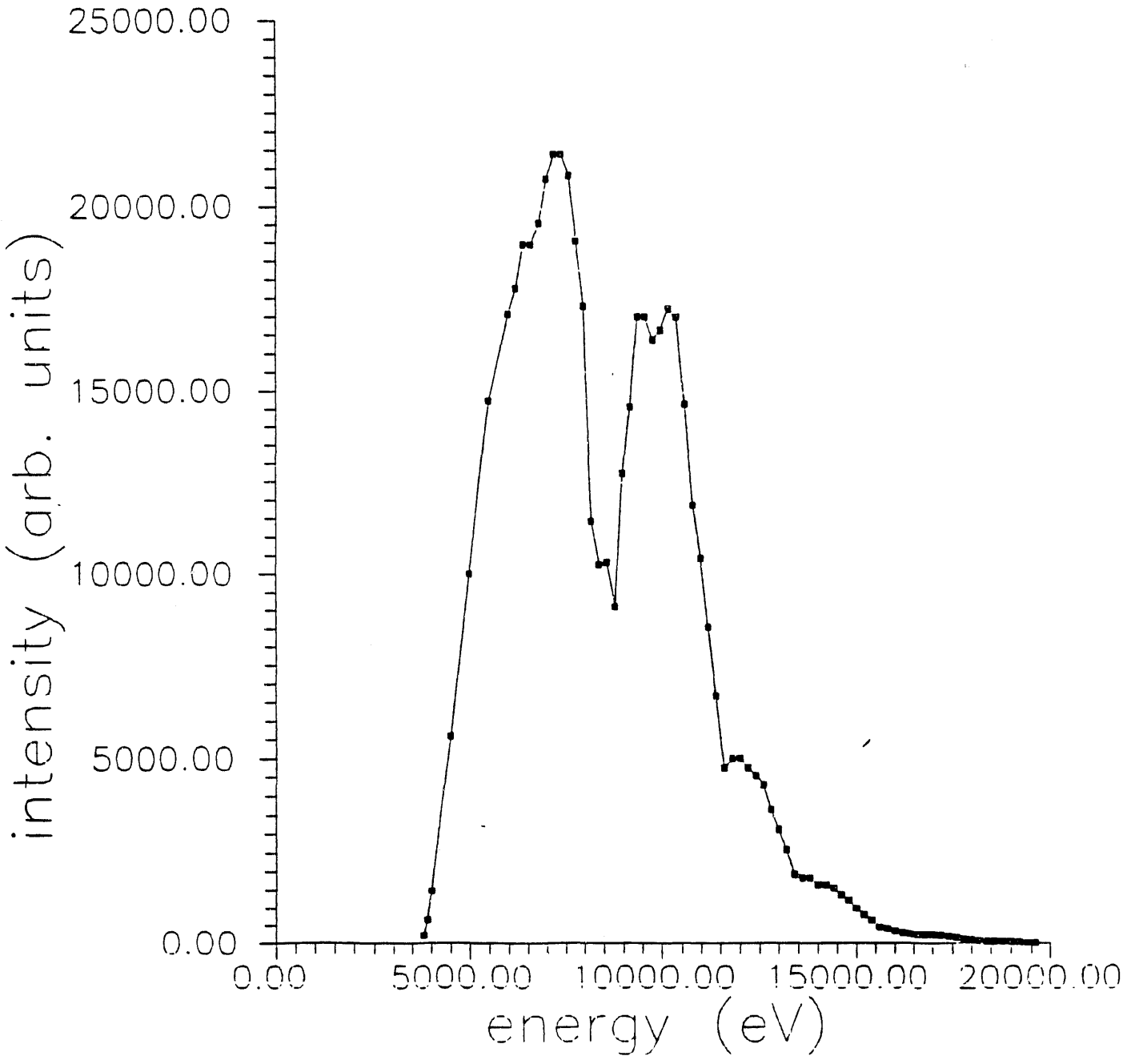
Beam Intensity with Focusing Mirror versus Energy
25000.00
20000.00
15000.00
10000.00
5000.00
0.00
intensity (arb. units)
0.00
5000.00
10000.00
15000.00
20000.00
energy (eV)

Figure B1

APPENDIX C

Focused Beam Cross-Section

The cross-section of the focused beam is shown in the horizontal and vertical in Figures C1 and C2 and was done in the following way. The ion chamber was mounted on the 2-theta arm with only one set of slits in use, these being mounted at the sample position, and was set to accept the direct beam. With these slits set at 2 mm wide in the horizontal and wide open in the vertical, the mirror angle was adjusted for maximum intensity. The slits were then set at 2 mm high in the vertical and wide open in the horizontal and the mirror bending was adjusted for maximum intensity. After this procedure, pictures were taken before, at, and after the slits position to be certain that the smallest beam, and therefore the focal point, was at the slits.

The slits were again mounted at the sample position. The vertical slit size was set at 0.2 mm, with the horizontal wide open, and this slit was scanned vertically to map out the cross-section of the focused beam in the vertical. The minimum cross-section achieved (the best focus) in the vertical was 0.510 mm FWHM. The horizontal slit size was then set at 0.2 mm, with the vertical wide open, and this slit was scanned horizontally to map out the cross-section of the beam in the horizontal. The minimum cross-section achieved in the horizontal was 1.1 mm FWHM.

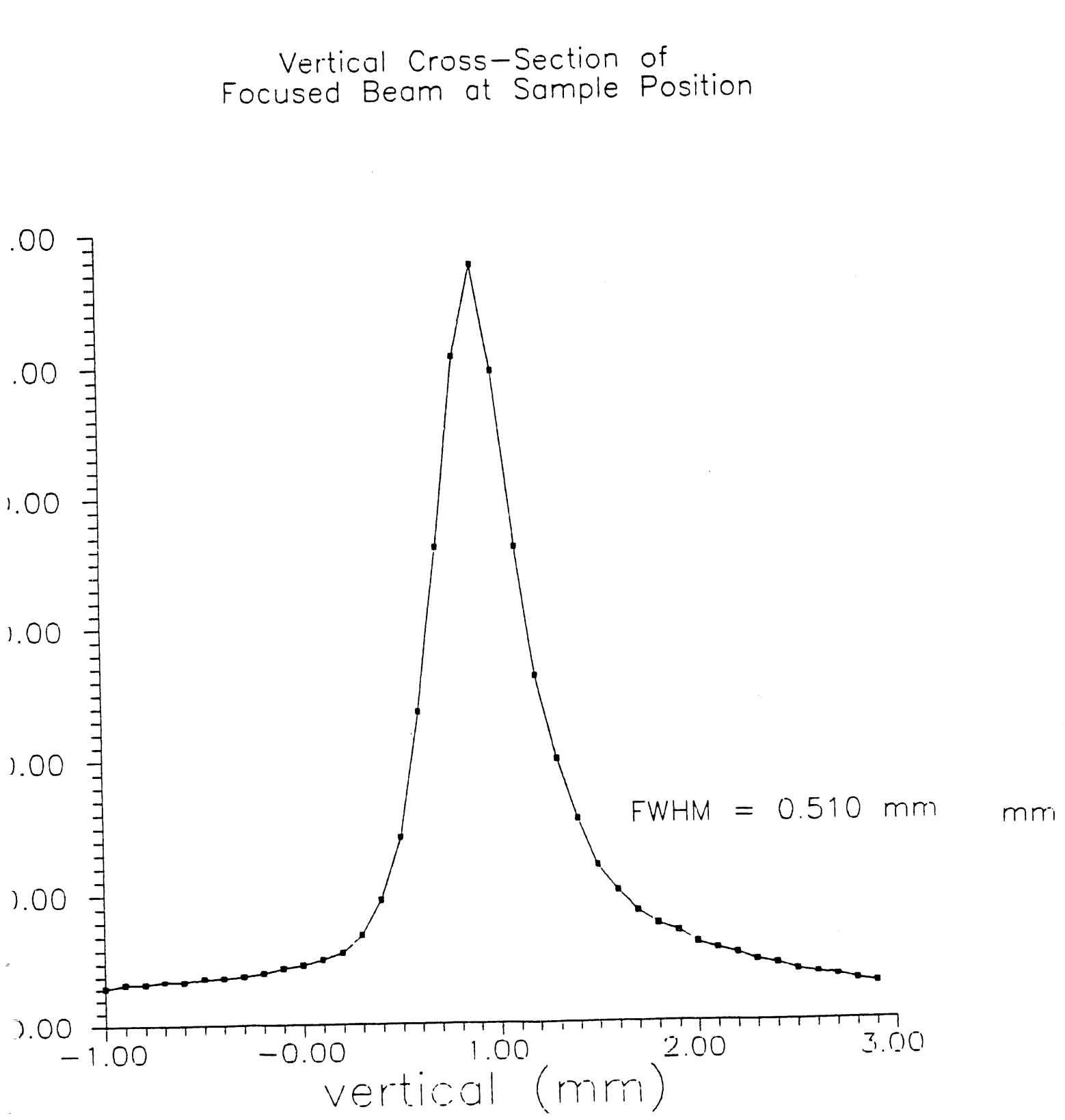
Vertical Cross-Section of
Focused Beam at Sample Position
.00
.00
).00
).00
).00
).00
FWHM = 0.510 mm
mm
-1.00
-0.00
1.00
2.00
3.00
vertical (mm)

Figure C1

APPENDIX D

Beam Divergence

The divergence of the focused beam was measured in the vertical and horizontal, at an energy of 4.3 keV, in the following way. A piece of single crystal Si, placed in a holder with a 1 mm diameter hole was mounted at the center of the diffractometer, and in the beam, so that the beam went through the hole. With $\chi = 0°$ and $2\theta = 0°$, phi was scanned until the Bragg condition for the (220) reflection was satisfied. The angular width over which anomalous transmission take place is a fraction of an arcsecond so that the width of the peak corresponds to the vertical divergence of the beam. This was repeated at $\chi = 90°$ to measure the horizontal divergence of the beam. These plots are shown in Figures D1 and D2. The measured divergence from the FWHM of these peaks is 0.2 milliradians in the vertical and 0.9 milliradians in the horizontal.

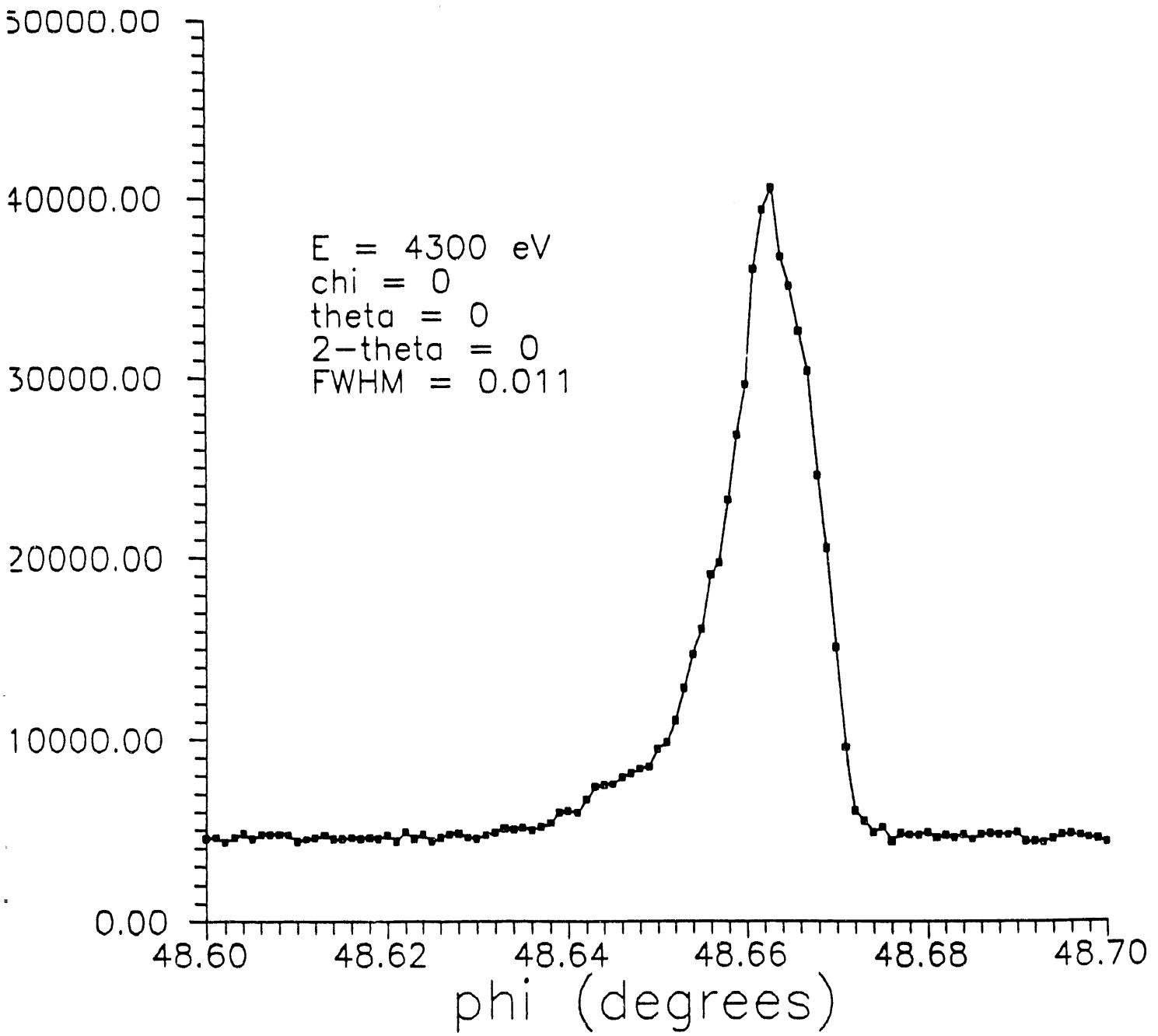
50000.00
40000.00
30000.00
20000.00
10000.00
0.00
E = 4300 eV
chi = 0
theta = 0
2-theta = 0
FWHM = 0.011
48.60
48.62
48.64
48.66
48.68
48.70
phi (degrees)

Figure D1

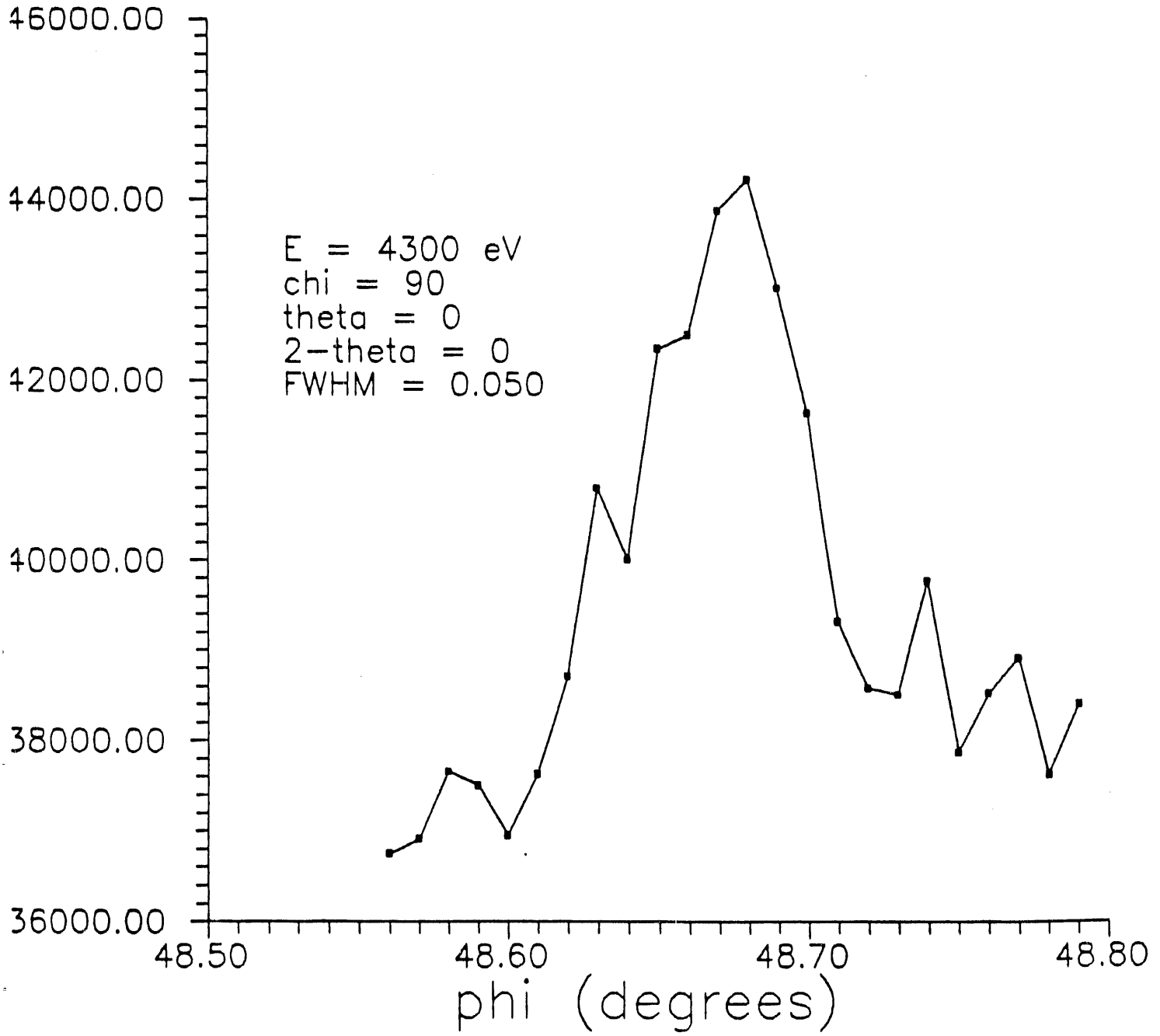
46000.00
44000.00
42000.00
40000.00
38000.00
36000.00
E = 4300 eV
chi = 90
theta = 0
2-theta = 0
FWHM = 0.050
48.50
48.60
48.70
48.80
phi (degrees)

Figure D2

APPENDIX E

Beam Stability

The beam stability, both in energy and in intensity, was measured by scanning repeatedly through the (111) reflection of a single crystal Ge sample for several hours. This was done with the focusing mirror in place. Each peak was then fitted for peak location and intensity. The peak location (Bragg angle) was then used to calculate the energy of the x-rays. This is plotted as a function of time in Figure E1. The integrated intensity is plotted as a function of time in Figure E2. The ring current is plotted as a function of time in Figure E3.

Reprints removed.

END

DATE
FILMED
3/19/92